An Early Byzantine Engraved Almandine from the Garibpet Deposit, Telangana State, India: Evidence for Garnet Trade Along the Ancient Maritime Silk Road

H. Albert Gilg, Karl Schmetzer, and Ulrich Schüssler

An Early Byzantine almandine garnet engraved with a Christian motif and dated to the late sixth to eighth century offers insight into trade practices in antiquity. The gemstone was characterized by a combination of nondestructive analytical methods including electron microprobe, portable X-ray fluorescence, Raman spectroscopy, and optical microscopy. The chemical composition and zoning, in combination with the inclusion assemblage and the distinct distribution of inclusions between an inclusion-rich core and an inclusion-poor rim, indicated that the sample most likely originated from the large Garibpet deposit in Telangana State, India. The Byzantine intaglio thus furnishes evidence of garnet transport from the eastern Indian coast to the Mediterranean world during Early Medieval times. In so doing, it supports the interpretation of a sixth-century text by the Greek merchant and traveler Cosmas Indicopleustes, which describes the export of "alabandenum," a reference to garnet, from harbors on the southeast Indian shore along the ancient Maritime Silk Road. This idea is further buttressed by considering that garnet from the Garibpet deposit was used for bead production at the archaeological site of Arikamedu, one of the historical ports on the Coromandel Coast in southeast India. Conversely, a comparison with properties of the two predominant types of almandine used in Merovingian cloisonné jewelry shows that the characteristic mineralogical features and therefore the sources of these garnets set in Early Medieval jewelry were different.

Red to purple garnets of predominantly pyrope, pyrope-almandine, and almandine compositions were highly esteemed and frequently employed for gemstone purposes in Hellenistic and Early Roman Imperial times, from about 300 BCE to 200 CE (e.g., Spier, 1989; Zwierlein-Diehl, 2007; Adams, 2011; Thoresen, 2017). With regard to fashioning, engraved gems were prominent during this era but became much rarer during Late Roman Imperial times of the third and fourth century CE (figure 1), signaling a decline in the art of gem engraving (e.g., Entwistle and Adams, 2011).

An apparent resurgence in the use of engraved gemstones occurred in the middle of the fifth century (Spier, 2007, 2011), and the period from the fifth to the seventh century saw developments spread across multiple localities and cultures. Depending on the focus and context, this period may be variously referred to as Early Byzantine, Early Medieval, or Merovingian, among others. Spier (2011), for instance, suggested the existence of a prolific garnet workshop associated with the Early Byzantine imperial court in Constantinople that specialized in engraving the hard red stone, as well as sapphire, during the fifth to the seventh century. The Early Byzantine garnets might thus serve to suggest a revival in the Hellenistic to Early Roman Imperial tradition of gem engraving. The earliest and finest examples displayed beautiful portraits, for example of Theodosius II, while the quality of later ob-

See end of article for About the Authors and Acknowledgments.
Gems & Gemology, Vol. 54, No. 2, pp. 149–165,
http://dx.doi.org/10.5741/GEMS.54.2.149

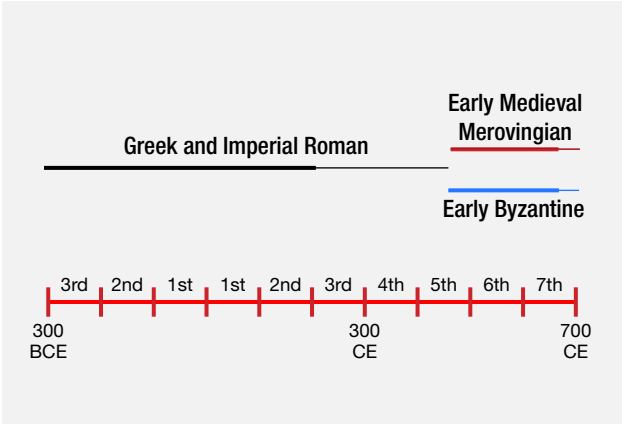

Figure 1. This schematic timeline shows the use of garnets in different eras within the so-called garnet millennium, from 300 BCE to 700 CE.

jects embellished with doves, eagles, dolphins, and religious images or symbols varied substantially. Notably, Early Byzantine engraved garnet seal stones comprised a significant proportion of Early Christian gems (Spier, 2007).

Garnets also played a significant role in Early Medieval (including Merovingian) cloisonné jewelry of the fifth to seventh century (e.g., Arrhenius, 1985; Calligaro et al., 2002; Gilg et al., 2010; Adams, 2014). Largely contemporaneous use of garnet during these centuries can likewise be seen with seal stones in pre-Islamic Persia and Central Asia (Adams, 2011; Adams et al., 2011; Ritter, 2017) and with transparent red beads produced for the Indo-Pacific trade network in the first millennium CE (Francis, 2002; Carter, 2012, 2013, 2016; Borell, 2017; Schmetzer et al., 2017). Evidence further suggests that manufacture of cloisonné jewelry may have begun with the use of non-engraved flat ring stones as garnet inlays for polychrome jewelry in the Black Sea region (Adams, 2011, 2014).

More than 4,000 individual garnets from Early Medieval cloisonné jewelry have been analyzed chemically, with the resultant data indicating classification into at least six garnet types, clusters, or groups with generally distinct features: three of almandine, two of pyrope, and one of intermediate pyrope-almandine with more variable chemical and inclusion characteristics (Quast and Schüssler, 2000; Calligaro et al., 2002, 2006-2007; Mannerstrand and Lundqvist, 2003; Périn and Calligaro, 2007; Mathis et al., 2008; Gilg et al., 2010; Horváth and Bendö, 2011; Gilg and Gast, 2012; Gast et al., 2013; Šmit et al., 2014; Bugoi et al., 2016; Périn and Calligaro, 2016). In contrast, less than 40 full chemical analyses of Hellenistic, Etruscan, and Roman garnets, mostly intaglios and cameos along with a few beads, have been published to date; these data were summarized by Thoresen and Schmetzer (2013). A portion of these stones demonstrated compositions that overlapped with some types found in Early Medieval cloisonné jewelry, but others reflected different chemistries, in particular a Ca- and Mn-rich, Mg-poor almandine (a fourth type or cluster of almandine), and likely derived from sources not used to supply the Medieval examples. Garnets from the Early Byzantine seal stones have not yet been analyzed or assigned to specific garnet types or clusters.

More recently, a detailed study on garnet beads from the Arikamedu archaeological site in Tamil Nadu State, India, identified a new (fifth) type of almandine used in antiquity (figure 2). The archaeological context of that site is described in detail by Schmetzer et al. (2017). The garnets were characterized by a distinct chemical composition with a conspicuous chemical zoning and a zonal distribution of inclusions. These features were shown to correspond with those of almandines from the alluvial Garibpet deposit in Telangana State, India (Schmetzer et al., 2017). The Garibpet locality was first described by Voysey (1833), and Bauer (1896) similarly mentioned it as a secondary occurrence of better-quality gem garnets in India. Production figures were then reported by Mirza (1937), covering a period from 1910 to 1929. In the current era, the prolific nature of the deposit has continued to be recognized, with literature describing a garnet-bearing schist that "constitutes an entire hill at Garibpet, in the Khammam

In Brief

- An engraved almandine garnet, dated to the late sixth to eighth century by art historians through comparison of its stepped-cross motif with Byzantine coinage, provides insight into trading practices in antiquity.
- Chemical composition and inclusion characteristics indicate that the gemstone originated from the Garibpet deposit in India. Garibpet has also been shown to have supplied the rough material for bead production at Arikamedu, an early port and trade center on the southeast Indian coast.
- A sixth-century Greek text describing export of "alabandenum" from the port of Caber, near Arikamedu, has been interpreted as a contemporaneous reference to shipping of almandine from the Coromandel Coast.
- The Byzantine gem serves as tangible evidence of garnet trade between India and the Mediterranean world along the Maritime Silk Road.

Figure 2. This map of southern India shows the locations of Garibpet and Arikamedu on the subcontinent, together with the ancient harbor of Kaveripattinam.

district" of Telangana State (Phani, 2014). Taken together, such references thus chronicle centuries of ongoing use of garnets from the deposit.

An extensive historical role can likewise be documented for Arikamedu, an important port, bead production site, and trading center along the Indian Ocean during the first millennium CE (Wheeler et al., 1946; Casal, 1949; Begley et al., 1996, 2004; Francis, 2004). Some have even equated Arikamedu with the harbor of Podouke (Podukê) mentioned in the *Periplus Maris Erythraei*, a sailing guide for merchants written by an anonymous author in the first century CE (Raman, 1991). Another important ancient harbor on the Indian east coast (the Coromandel Coast), south of Arikamedu, was Kaveripattinam (Rao, 1991a,b; Gaur and Sundaresh, 2006; Sundaresh and Gaur, 2011). The Kaveripattinam port has been associated with the Kaberis Emporium cited by Ptolemy (Raman, 1991) and with a locality referred to as "Caber" by the Greek traveler and merchant Cosmas Indicopleustes in his mid-sixth century CE text known as *Christian Topography* (Banaji, 2015; an English translation is available from Winstedt, 1909, and a modern edition with commentary from Schneider, 2011). It has been speculated that the text mentioning "Caber, which exports alabandenum" refers to shipment of almandine

Figure 3. Early Byzantine garnet intaglio with a stepped-cross motif, dated from the late sixth to eighth century CE. The stone measures 10.1 × 6.1 mm and weighs 1.95 ct. Reflected light. Photo by K. Schmetzer.

garnet (Roth, 1980; Kessler, 2001) on the ancient Maritime Silk Road (see Ptak, 2007).

To date, interpretation of the above-cited sixth-century text has remained obscure, principally because no direct evidence of Garibpet garnets being used in the Mediterranean world during the fifth to seventh or even eighth century CE has been reported. With the aim of probing this question, the present study of an Early Byzantine garnet intaglio (figure 3) was undertaken. Chemical composition and inclusion characteristics were examined using nondestructive methods. Properties from this sample were then compared with those of rough garnets from the Garibpet secondary deposit and fashioned almandines from Merovingian cloisonné jewelry.

MATERIAL AND METHODS

The subject intaglio has been maintained in a private collection (Christian Schmidt, Munich, inventory number 2847) and is said to be from Israel. The sample was previously described by Spier (2011) as catalogue addition No. 58, plate 37. It came to the attention of author HAG while investigating a series of engraved historical garnets from various collections. After a preliminary examination of the sample's inclusion pattern that revealed features typical of garnets from the Garibpet deposit, a more detailed study followed. As all analyses of the engraved gemstone had to be performed by nondestructive methods, only portable X-ray fluorescence (p-XRF) and electron microprobe analysis were employed for determining the major, minor, and trace-element contents. Application of micro-destructive techniques, such as laser ablation–inductively coupled plasma–mass spectrometry (LA-ICP-MS), was not possible.

Chemical analysis was initially achieved with a handheld Niton XL3t XRF analyzer by Thermo Fisher Scientific, which was equipped with a silver anode and a helium purging system. The analysis was performed in the bulk mode ("mining mode") with a collection time of 120 s, using four different settings for acceleration voltage and beam current. The analytical spot size of the primary X-ray beam was in the range of 4 × 3 mm, with the beam directed toward the inclusion-poor side of the gem. The data provided by the automated software were calibrated using a set of approximately 30 gem-quality garnets that had previously been analyzed by electron microprobe, particle-induced X-ray emission (PIXE), and LA-ICP-MS, normalized to 100 wt.%. The detection limits were ~1 wt.% for MgO; ~100 ppm for Ti, Cr, and V; ~50 ppm for Zn; and ~25 ppm for Zr and Y.

Electron microprobe analysis was carried out on a JEOL JXA 8800L microprobe with wavelength-dispersive channels. Analytical conditions were as follows: 15 kV accelerating voltage, 20 nA beam current, 1 µm beam diameter, and counting times of 20 s for peak positions and 20 s for background. Natural and synthetic silicate and oxide mineral standards or pure element standards supplied by Cameca were used for calibration (i.e., andradite for Si and Ca, hematite for Fe, Cr_2O_3 for Cr, corundum for Al, $MnTiO_3$ for Mn and Ti, and MgO for Mg). Kα radiation was utilized in the process. Matrix correction was performed by a ZAF procedure. Under these conditions, the detection limit was ~0.05 wt.% for most elements, and the analytical precision was better than 1% relative for all major elements. The proportion of end members was calculated from the chemical analyses using the methods of Locock (2008).

Optical investigations and documentation were performed with a Schneider immersion microscope with Zeiss optics, a Leica DM LM polarizing micro-

Figure 4. The Early Byzantine garnet intaglio displays an inclusion-rich core, slightly decentered to the right side of the stepped cross, and a more transparent rim. Three areas analyzed by electron microprobe are marked C (core), R (rim), and I (intermediate zone). Transmitted light. Photo by H.A. Gilg.

scope with transmitted and reflected light sources, and an Olympus stereomicroscope, the latter two both equipped with an Olympus DP25 digital camera and Olympus Stream Motion software. Selected mineral phases were identified by micro-Raman spectroscopy using a Horiba Jobin Yvon XploRA PLUS confocal Raman microscope. The spectrometer was equipped with a frequency-doubled Nd:YAG laser (532 nm, with a maximum power of 22.5 mW) and an Olympus LMPLFLN 100× long-working-distance objective with a numerical aperture of 0.9.

PROPERTIES OF THE ENGRAVED ALMANDINE AND COMPARISON WITH GARNETS FROM THE GARIBPET DEPOSIT

Visual Appearance. The historical garnet (figure 3) was red and had been fashioned as an oval, strongly convex cabochon with a concave back. The cabochon measured 10.1 × 6.1 mm, with a height of 4.4 mm from the base to the tip of the dome, and weighed 1.95 ct. The gemstone depicted a simple cross with three steps, and the presence of specific grooves indicated that the design had been engraved using a wheel. This stepped-cross motif—probably depicting the bejeweled cross of Theodosius II at Golgotha—first appeared in Byzantine coinage at the end of the sixth century, in solidi of Roman Emperor Tiberius II Constantine, but the design was also common in the seventh and eighth centuries (Brubaker and Haldon, 2001; Brubaker, 2012). Accordingly, gemstones engraved with this motif can be dated to the period from the late sixth to the eighth century (Spier, 2011). The main usage of garnets in this period, however, is related to the sixth and seventh century, with a decline in the second half of the seventh and a rapid decline in the eighth century (J. Spier, pers. comm., 2018).

The garnet showed a slightly decentered inclusion-rich area (core) that was surrounded by an inclusion-poor, more transparent zone (rim). A small fracture with brownish secondary staining was also seen (figures 3 and 4).

Chemical Composition. Three areas on the convex side of the intaglio were examined chemically via electron microprobe, with several point analyses in each area. Analysis positions are indicated in figure 4. These included the central part of the inclusion-rich core (C); the inner part of the more transparent, inclusion-poor rim (R); and an intermediate area (I) located between the core and the rim. Due to the uneven form of the cabochon, a separate mounting of the garnet was necessary for each sequence. Analyses of a given area that totaled between 98 and 101 wt.% oxides signaled acceptable analytical results, despite the difficult measurement geometry of the curved surface. Analyses below 98 wt.% oxides, stemming either from the uneven surface or from inclusions struck by the electron beam, were rejected. The results are summarized in table 1 and compared with chemical properties of garnets from Garibpet and from Merovingian cloisonné jewelry (see below) in table 2.

The electron microprobe analyses revealed that the engraved gem was a member of the pyrope-almandine

TABLE 1. Chemical properties of the Early Byzantine engraved gemstone from this study.

Sample	Position, electron microprobe analyses			Position, portable X-ray fluorescence analysis
	Major and minor element content, compositional ranges (oxides in wt.%)			
Details	Core, 3 analyses	Intermediate Zone, 9 analyses	Rim, 5 analyses	Rim, 1 analysis
SiO_2	34.96–36.06	35.03–36.50	35.80–36.51	35 ± 2
TiO_2	0.01–0.02	0.00–0.04	0.00–0.05	<0.1
Al_2O_3	20.92–21.67	20.73–21.85	21.26–21.85	20 ± 2
Cr_2O_3	0.02–0.06	0.00–0.04	0.01–0.07	<0.1
Fe_2O_3*	2.57–4.08	1.57–3.03	1.31–2.46	
MnO	1.30–1.35	1.20–1.33	1.13–1.22	1.3 ± 0.3
MgO	2.48–2.63	2.49–2.69	2.56–2.67	<3
CaO	0.68–0.69	0.66–0.70	0.61–0.65	0.9 ± 0.3
FeO*	35.20–36.20	35.71–36.90	36.22–36.87	
FeO_{total}	37.98–38.62	37.69–38.55	38.05–38.60	45 ± 7
	Molecular percentages of end members (ranges, in mol.%)**			
Almandine	80.07–81.49	81.03–82.18	81.49–82.41	
Pyrope	10.12–10.48	10.31–10.72	10.29–10.64	
Spessartine	3.03–3.12	2.74–3.01	2.59–2.70	
Grossular	1.75–1.92	1.53–1.94	1.44–1.80	
Andradite	0.20–1.51	0.10–0.24	0.21–0.44	
	Trace-element content (ppm)			
Y				312
Zn				111
Zr				<25
V				<100
Cr				<100
Ti				<100

** Fe_2O_3 and FeO calculated from stoichiometry*
*** Using the scheme of Locock (2008), the calculated remainder is between 2.4 and 3.8%.*

solid solution series, with almandine between 80.1 and 82.2 mol.% and relatively low pyrope between 10.1 and 10.7 mol.%. Minor percentages of spessartine between 2.6 and 3.1 mol.% and of grossular between 1.4 and 1.9 mol.% were also found (table 1). Ti and Cr were below the detection limit of the electron microprobe. The chemical composition was within the compositional field for garnets from Garibpet (table 2 and figure 5).

The intaglio was chemically zoned, with slightly elevated Mn and thus higher spessartine percentages in the core than in the rim (figure 5, right). A similar Mn zoning was characteristic of Garibpet almandines. A weak zoning of Ca, also observed in some of the Garibpet garnets, was apparent in the engraved gemstone, with slightly higher values in the core and in the intermediate zone than in the rim (figure 5, left). These data on major element zoning were indicative of prograde metamorphic growth (see, e.g., Spear, 1993).

X-ray fluorescence analysis provided meaningful results only for the inclusion-poor rim of the engraved garnet. The data confirmed the average major elemental composition as determined by electron microprobe, especially the low Ca and moderate Mn, but showed considerable uncertainties with respect to Mg, Si, Al, and Fe due to the unfavorable geometry during analysis. The XRF analysis also demonstrated high concentrations of Y (~300 ppm) and Zn (~100 ppm), while Zr, V, Cr, and Ti were below the detection limit of the instrument (table 1). Due to the large spot size and the abundance of inclusions in the core, it was not possible to detect any trace-element zon-

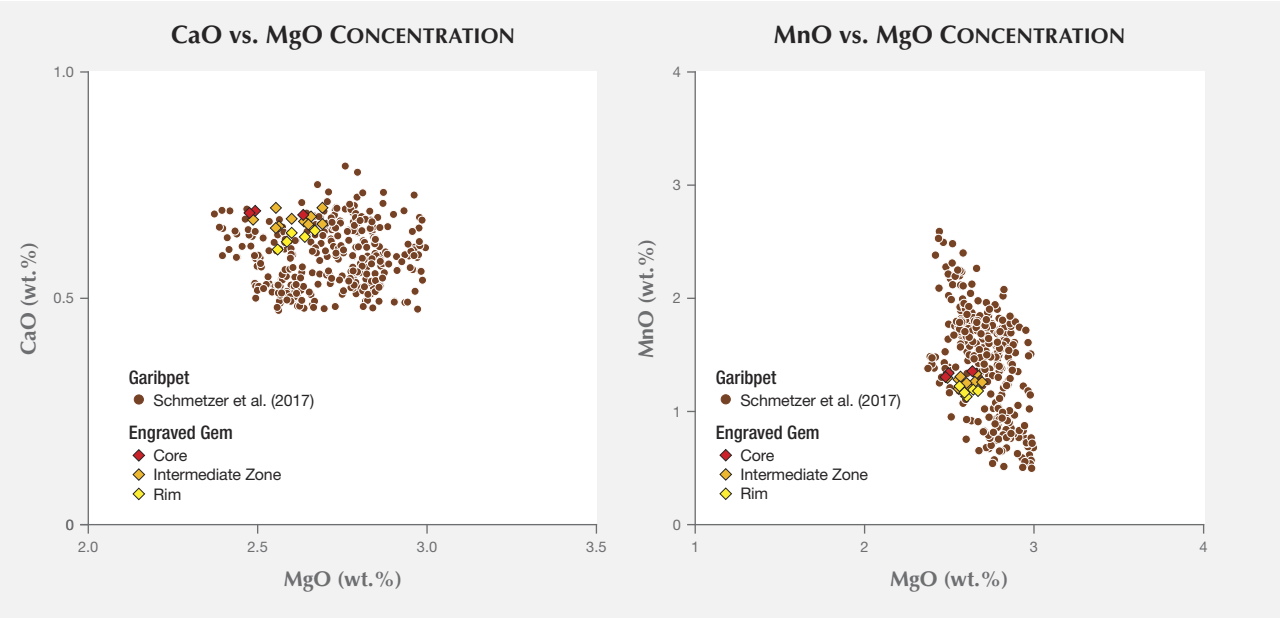

Figure 5. Binary plots showing the chemical composition of the engraved Byzantine garnet and samples from Garibpet as MgO, CaO, and MnO weight percentages.

ing. The high Y and Zn contents and low Zr, V, Cr, and Ti concentrations of the engraved gem were fully consistent with the values reported for Garibpet garnets on the basis of LA-ICP-MS data (table 2).

Microscopic Characteristics. Characteristic inclusions observed in the engraved gem, as well as those seen in garnets from the Garibpet deposit and detailed by Schmetzer et al. (2017), are presented in figures 6 and 8; an overview is provided in table 3.

The gem displayed conspicuous zoning with an inclusion-poor, transparent rim and an inclusion-rich translucent core that was slightly decentered to the right side of the oval (figures 3, 4, and 6A). The translucent core encapsulated a variety of minerals, some of which were opaque and hindered the visibility of the core zone and occasionally the identification of the minerals.

Four types of inclusions proved dominant. A particularly characteristic inclusion feature was the presence of aggregates of curved colorless sillimanite fibers at the border between the inclusion-rich core and the inclusion-poor rim (figure 8E). The other three dominant inclusion types were seen principally within the core, as described below.

Opaque, mostly anhedral elongate crystals (figure 6C) were a prominent core feature and were in part aligned following a schistosity. These irregularly shaped minerals with rounded surfaces were identified as ilmenite by their Raman spectrum. Some Raman spectroscopic measurements also yielded bands characteristic of rutile (444 and 607 cm^{-1}), indicating rutile overgrowth on the ilmenite.

Another common core inclusion was a transparent, colorless, isometric to slightly elongate or irregularly shaped mineral that showed a maximum size of up to several hundred µm (figure 6E). The crystals were identified as quartz by a typical Raman spectrum with a main band at approximately 464 cm^{-1}. Quartz also occurred rarely in the inclusion-poor rim.

Other common inclusions in the core were long-prismatic, partially segmented apatite crystals with rounded edges that could reach a length of more than 200 µm. Included within these crystals were abundant opaque flakes (figure 6G). The small euhedral flakes, approximately 10 µm in diameter, were identified by Raman spectroscopy as graphite (figure 7). The prominent G band at 1580 cm^{-1} in the first-order region and the second-order bands between 2400 and 3300 cm^{-1} were very sharp, while the D1 band was poorly developed, thus signaling high-temperature growth conditions of at least 600°C (Wopenka and Pasteris, 1993; Beyssac et al., 2002).

Notably, the four dominant features just described matched those found in Garibpet garnets (see Schmetzer et al., 2017). The sillimanite fibers between the core and rim were the signature inclusion feature observed in Garibpet garnets and in beads from Arikamedu (Schmetzer et al., 2017), with an

TABLE 2. Comparison of chemical features in the Early Byzantine engraved gemstone, garnets from the Garibpet deposit, and Cluster A and B almandines from Merovingian cloisonné jewelry.

Sample	Engraved gem	Garibpet	Cluster A [Type II]	Cluster B [Type I]
Major and minor elements	**Mean values with standard deviation [ranges], in wt.%**			
Analytical technique, number of analyses	EMPA, n = 17[1]	EMPA, n = 329[2]	EMPA, n = 28[3] PIXE, n = 175[5]	EMPA, n = 85[3] PIXE, n = 491[5]
SiO_2	35.82 ± 0.48 [34.96–36.51]	36.05 ± 0.34 [34.74–36.84]	37.78 ± 1.04 [34.19–39.62]	37.26 ± 0.55 [35.77–38.61]
			37.52 ± 0.66 [36.09–39.84]	36.83 ± 0.48 [36.00–37.98]
Al_2O_3	21.43 ± 0.35 [20.73–21.85]	21.54 ± 0.22 [20.55–22.24]	21.62 ± 0.64 [19.14–22.73]	21.14 ± 0.37 [20.36–22.31]
			21.65 ± 0.44 [20.36–23.35]	21.28 ± 0.33 [20.28–22.36]
MnO	1.25 ± 0.07 [1.16–1.35]	1.44 ± 0.45 [0.50–2.58]	1.26 ± 0.76 [0.13–3.17]	0.30 ± 0.24 [0.00–1.10]
			1.50 ± 0.85 [0.00–4.42]	0.25 ± 0.22 [0.00–1.28]
MgO	2.59 ± 0.07 [2.48–2.69]	2.72 ± 0.15 [2.37–2.99]	6.83 ± 1.00 [5.05–8.87]	4.71 ± 0.67 [3.29–6.26]
			6.49 ± 0.74 [4.46–9.07]	4.69 ± 0.66 [3.04–6.53]
CaO	0.66 ± 0.02 [0.61–0.69]	0.59 ± 0.07 [0.47–0.73]	1.46 ± 0.21 [0.96–2.01]	0.63 ± 0.16 [0.32–1.03]
			1.30 ± 0.20 [0.72–2.01]	0.63 ± 0.15 [0.32–1.03]
FeO_{total}	38.22 ± 0.26 [37.69–38.62]	37.72 ± 0.52 [36.30–39.21]	31.00 ± 1.02 [28.41–31.94]	36.11 ± 1.00 [33.49–37.75]
			31.24 ± 1.39) [26.52–35.63]	36.10 ± 1.13 [32.98–38.35]
Trace elements	**Mean values with standard deviation [ranges], in ppm**			
Analytical technique, number of analyses	p-XRF, n = 1[1]	LA-ICP-MS, n = 31[2]	PIXE, n = 175[5]	PIXE, n = 491[5]
Y	312	213 ± 70 [45–401]	534 ± 325 [57–1478]	57 ± 56 [0–416]
Zn	111	107 ± 15 [77–129]	34 ± 31 [0–369]	14 ± 30 [0–432]
Zr	<50	4 ± 2 [1–11]	26 ± 96 [0–1084]	7 ± 7 [0–34]
V	<100	28 ± 6 [17–44]	72 ± 30 [0–159]	10 ± 14 [0–86]
Cr	<100	55 ± 42 [25–255]	444 ± 165 [101–995]	7 ± 15 [0–121]
Ti	<150	38 ± 9 [18–55]	126 ± 75 [0–441]	74 ± 43 [0–257]
Chemical zoning	**Yes** **[Mn,Ca][1]**	**Yes** **[Mn,Ca,Zn][2]**	**Yes** **[Y][4]**	**Not described**

[1]*This study*
[2]*Schmetzer et al. (2017)*
[3]*Quast and Schüssler (2000)*
[4]*Calligaro et al. (2006-2007)*
[5]*Gilg et al. (2010)*

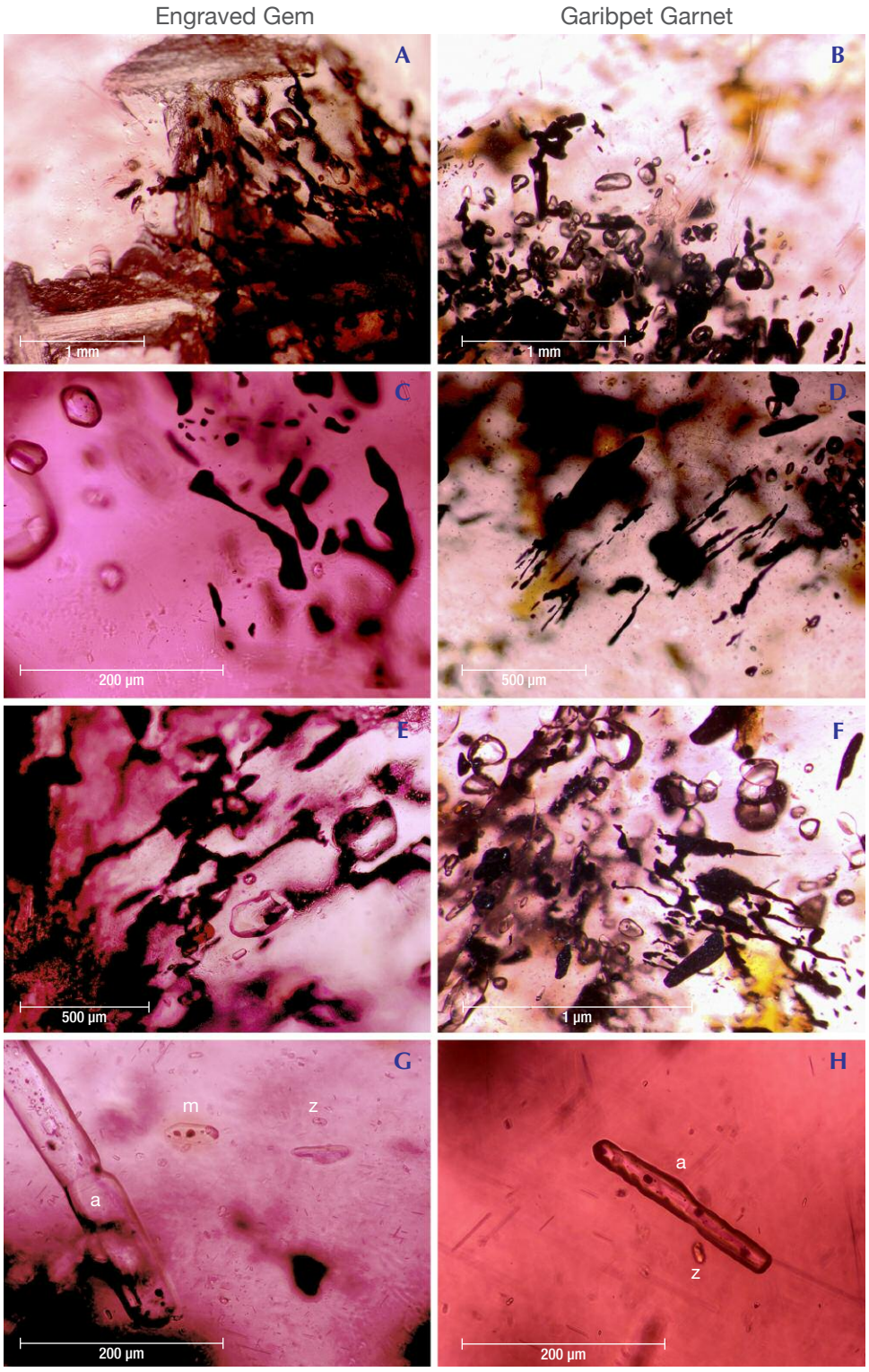

Figure 6. Comparison of inclusions in the Early Byzantine engraved gem (left) with garnets from the Garibpet deposit (right). A and B: Inclusion-rich core and inclusion-poor rim with sillimanite fibers at the boundary. C and D: Irregularly shaped ilmenite. E and F: Subrounded quartz crystals. G and H: Large long-prismatic apatite crystal (a) with characteristic graphite inclusions, along with short-prismatic zircon (z) and monazite (m) crystals. Photomicrographs by H.A. Gilg.

identical distribution and shape (figures 6B, 8F). The ilmenite, quartz, and long-prismatic graphite-bearing apatite were also typical for Garibpet stones (figure 6D, F, H; Schmetzer et al., 2017).

Turning to less dominant but still frequent inclusions in the engraved gemstone core, two types should be mentioned. One consisted of very small, transparent short-prismatic zircon crystals that

TABLE 3. Comparison of inclusion characteristics in the Early Byzantine engraved gemstone, garnets from the Garibpet deposit, and Cluster A and B almandines from Merovingian cloisonné jewelry.

Sample	Engraved gem (this study)	Garibpet (Schmetzer et al., 2017)	Cluster A [Type II][1]	Cluster B [Type I][1]
Inclusions	**Frequency**			
Ilmenite	+++	+++	+++	
Quartz	+++	+++	+++	
Biotite	+	+	+	
Chlorite in fluid inclusions		+	+	++
Apatite, euhedral, inclusion-rich	+++	+++		
Apatite, anhedral, green				+++
Rutile, needle network, coarse			+++	
Rutile, needle network, patchy	+	+		+
Rutile, short prismatic	+	+	+	
Sillimanite bundles at core-rim boundary	+++	+++		
Sillimanite, individual coarse needles		+	++	
Monazite	++	++	++	++
Zircon	++	++	+++	+
Uraninite				++
Graphite in apatite	+++	+++		
Graphite in monazite	++	++	++	++
Graphite	+		+	
Goethite in fractures	+	+	+	+

+++ dominant, ++ frequently present, + occasionally observed
[1]Gilg et al. (2010), Horváth and Bendö (2011), Gilg and Hommrichhausen, unpublished research

caused tension cracks in the host garnet (figure 6G). Another was found as irregularly shaped monazite crystals less than 50 µm in diameter and surrounded by distinctive brownish halos related to radiation damage. The monazites often contained opaque graphite and quartz inclusions as well (figures 6G, 8A). Both zircon and monazite, which are radioactive minerals, were also common in Garibpet garnets and displayed similar habits in that material (figures 6H, 8B).

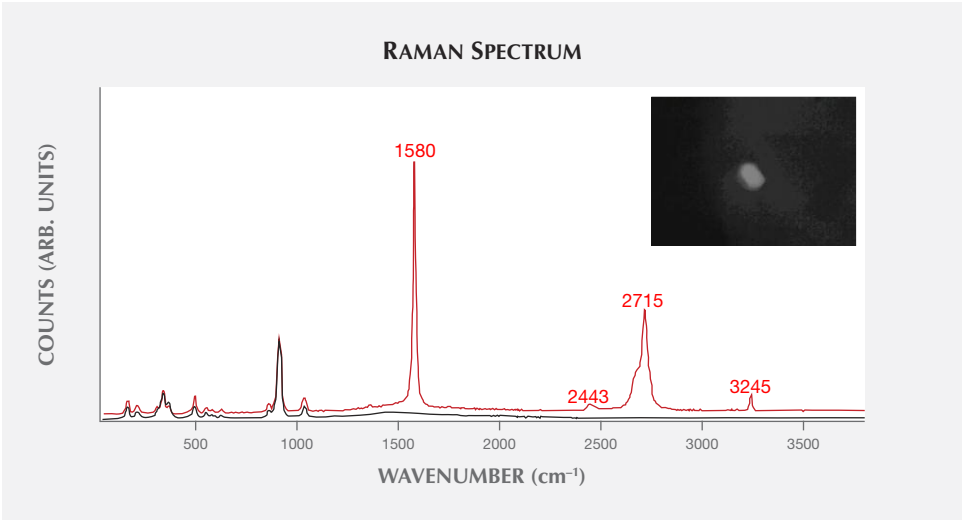

Figure 7. Raman spectrum of a graphite inclusion (red) and the host garnet (black) in the core of the engraved gem. The inset shows the size and shape of the graphite, appearing as a bright crystal in the center, in reflected light. Photomicrograph by H.A. Gilg.

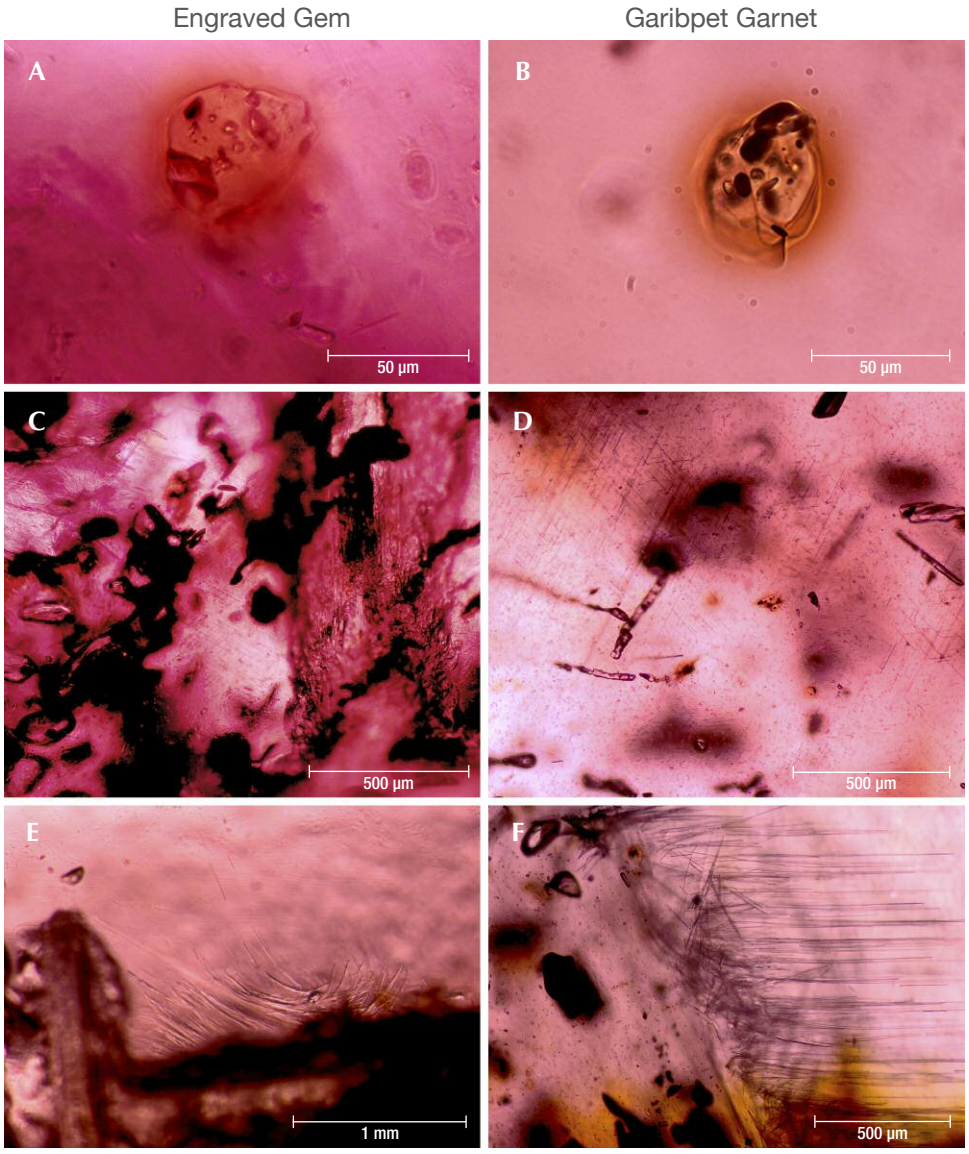

Figure 8. Comparison of additional inclusions in the Early Byzantine engraved gem (left) with garnets from Garibpet (right). A and B: Monazite with graphite and quartz inclusions. C and D: Patchy network of oriented rutile needles. E and F: Sillimanite fibers at the boundary between the inclusion-rich core and the inclusion-poor rim. Photomicrographs by H.A. Gilg.

Less frequently, a three-dimensional network of very thin rutile needles ("silk") was irregularly distributed in a patchy manner within the core zone of the engraved garnet (figure 8C). Such distribution of rutile needles was similar to a feature observed in about 10–15% of the Garibpet garnets (figure 8D).

A rare brown platy crystal approximately 150 µm in length was attached to an ilmenite crystal in the engraved Byzantine garnet (figure 9, top). It resembled short prismatic rutile crystals found overgrown on ilmenite in some Garibpet garnets (see figure 26D in Schmetzer et al., 2017), but the mineral was identified here as biotite on the basis of its Raman spectrum, with an OH-stretching band at about 3664 cm^{-1} (figure 9A; Wang et al., 2015). Meanwhile, with some further study of inclusion characteristics, biotite flakes have also been identified in samples from both Garibpet and Arikamedu (figure 9, bottom). Biotite is considered a less common accessory inclusion mineral found in Garibpet materials.

In the inclusion-poor rim of the engraved garnet, only a few quartz and zircon crystals and a brownish goethite-bearing fracture were observed (figure 4).

COMPARISON WITH CALCIUM-POOR ALMANDINES USED IN CLOISONNÉ JEWELRY

In contrast to the broad equivalence between the chemical and inclusion features of the Early Byzantine engraved garnet and garnets from the Garibpet deposit, comparison with the two dominant Ca-poor almandine types in Merovingian cloisonné jewelry

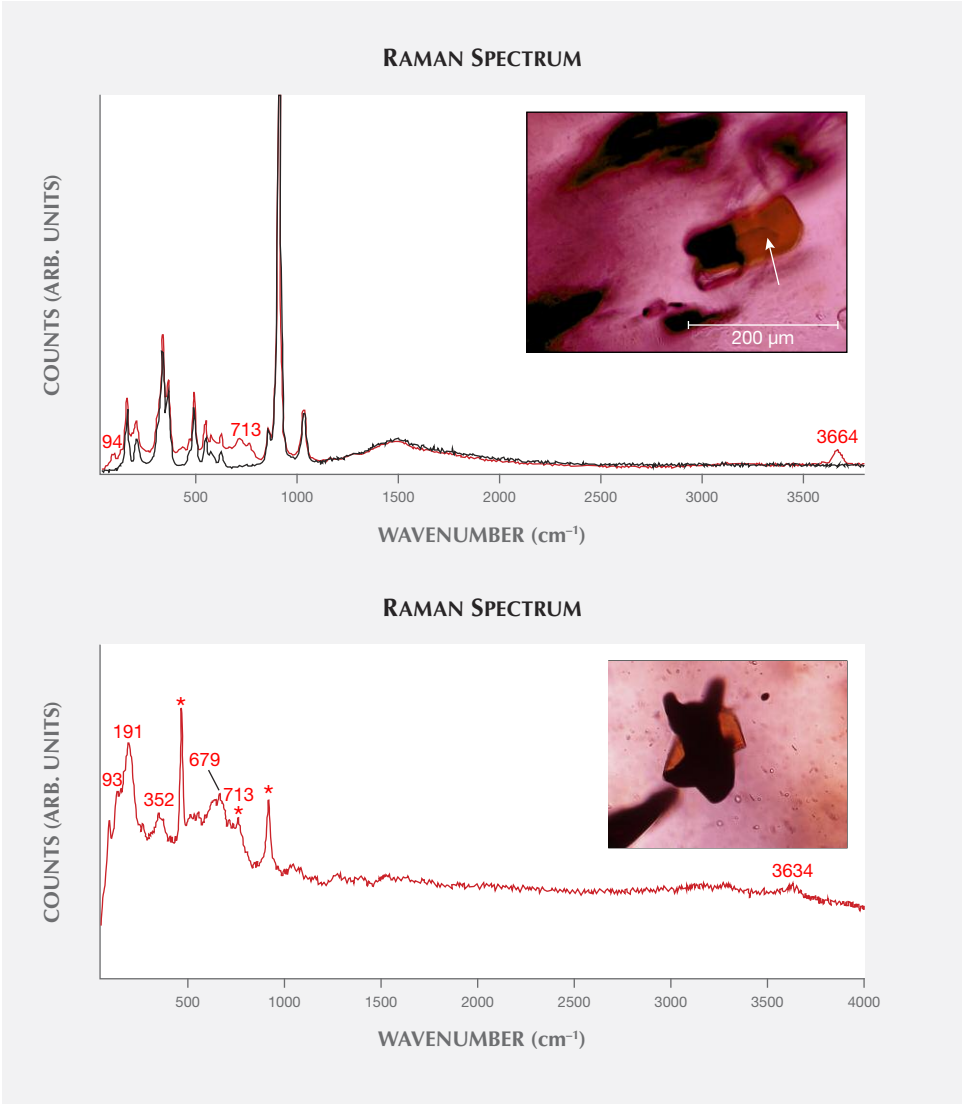

Figure 9. Top: Raman spectrum of a brownish biotite inclusion (red) and the host garnet (black) in the core of the engraved gem. The inset shows the size and shape of the biotite crystal, which is attached to an opaque ilmenite flake; the tip of the arrow shows the analysis spot. Bottom: Raman spectrum of a brownish biotite inclusion (red, the three peaks marked with an asterisk (*) are related to the host garnet) in a garnet from Garibpet, India. The inset shows the size and shape of the biotite crystal, which is attached to an opaque ilmenite. Photomicrographs by H.A. Gilg.

(Cluster A and Cluster B of Gilg et al., 2010, which are identical to Type II and Type I, respectively, of Calligaro et al., 2002) revealed substantially greater divergence. Again, tables 2 and 3 summarize these results.

Chemical Composition. As explained above, the composition of the Early Byzantine gemstone overlapped for all elements with the Ca-poor garnets from the Garibpet deposit. Conversely, considerably lower almandine and higher pyrope contents were measured for the two Ca-poor almandine types (Cluster A and Cluster B) in cloisonné jewelry (figures 10 and 11). Moreover, the high MnO, Y, and Zn levels found in the intaglio demonstrated inconsistency with Cluster B garnets, while the lower CaO, low Cr, and high Zn were incompatible with Cluster A garnets.

The low Ca content of the engraved gem further excluded any meaningful similarity with Ca-rich almandines, such as the Cluster C garnets observed in Scandinavian Early Medieval cloisonné jewelry (Löfgren, 1973; Mannerstrand and Lundqvist, 2003; Gilg and Hyršl, 2014) or the Ca- and Mn-rich almandines commonly encountered among Hellenistic or Early Roman engraved gems (Gilg and Gast, 2012; Thoresen and Schmetzer, 2013).

Microscopic Characteristics. A zonal arrangement of inclusions with an inclusion-rich core and an inclusion-poor rim has not been reported for either of the two Ca-poor Merovingian almandine types. Likewise, bundles of sillimanite fibers at a boundary between the core and rim portions have not been observed in either Cluster A or Cluster B garnets. Coarse silliman-

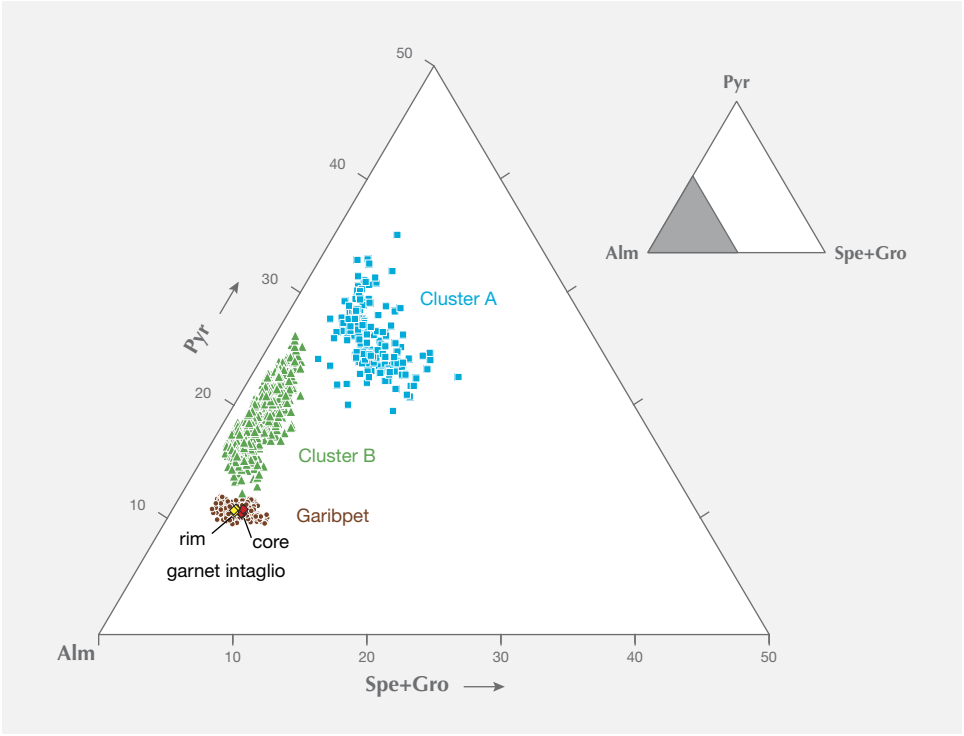

Figure 10. Triangular diagram of the chemical composition in molecular percentages (mol.%) of the core (red diamonds) and the rim (yellow diamonds) of the Early Byzantine garnet intaglio, in comparison with rough from the Garibpet deposit (brown circles, data from Schmetzer et al., 2017) and Cluster A and B almandines from Early Medieval cloisonné jewelry (blue squares and green triangles, respectively; data from Quast and Schüssler, 2000, and Gilg et al., 2010). Alm = almandine, Pyr = pyrope, Spe = spessartine, Gro = grossular.

ite needles, however, have been described for Cluster A almandines (figure 12C), but they were located within rather than bordering inclusion-rich zones, and none have been seen in Cluster B almandines (Calligaro et al., 2006-2007; Horváth and Bendö, 2011; Gast et al., 2013).

Two other dominant inclusions found in both the engraved garnet and the Garibpet material, ilmenite

Figure 11. Binary plots comparing the chemical composition of the garnet intaglio, with Garibpet rough and Cluster A and B almandines as MgO, CaO, and MnO weight percentages.

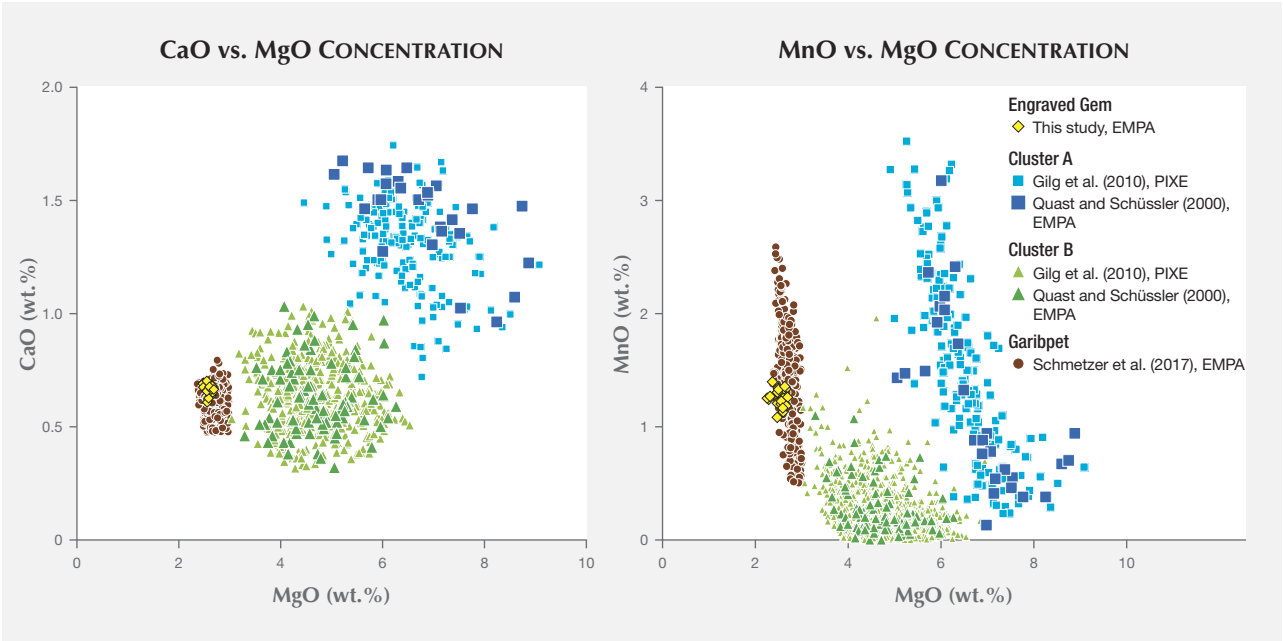

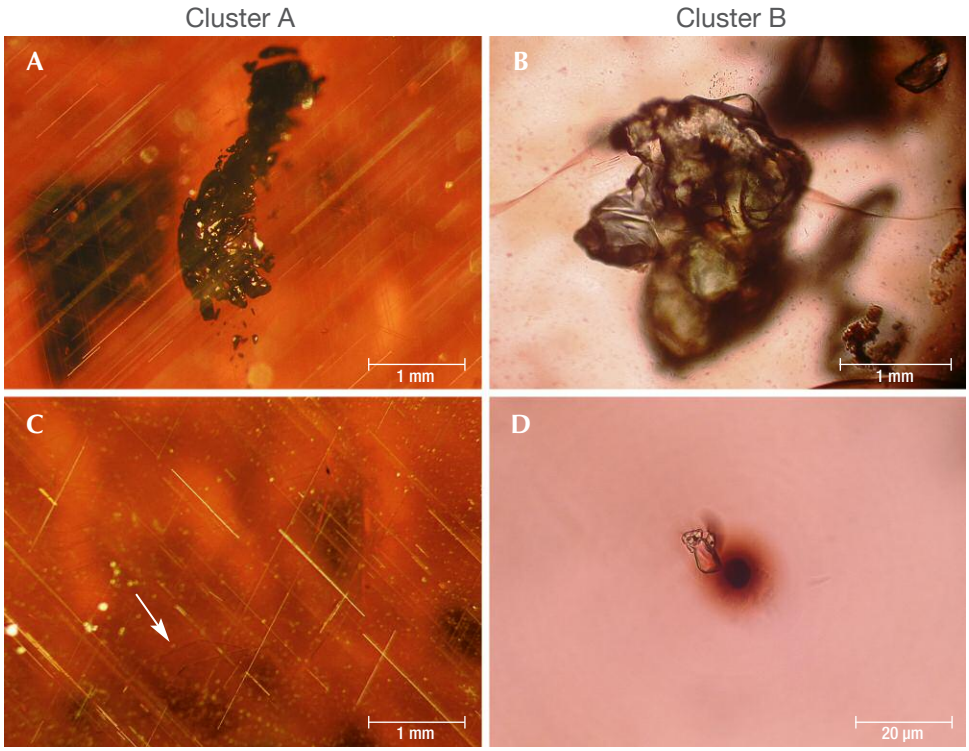

Figure 12. Characteristic inclusions in Ca-poor almandines from Merovingian jewelry of Cluster A (left) and Cluster B (right). A: Irregularly shaped ilmenite and acicular rutile network. B: Greenish xenomorphic apatite. C: Curved sillimanite needles (arrow) and rutile network. D: Black uraninite inclusion with brown radiation halo, along with colorless crystals of apatite (largest grain) and zircon (small grains with tension cracks). Photomicrographs by N. Hommrichhausen (A and C) and H.A. Gilg (B and D).

and quartz, have been reported with similar habits in Cluster A garnets (figure 12A) but have not been seen in Cluster B samples (Calligaro et al., 2002, 2006-2007; Gilg et al., 2010).

Apatite has been identified as a dominant inclusion in Cluster B garnets but has proven extremely rare in Cluster A samples (Calligaro et al., 2002, 2006-2007; Gilg et al., 2010). Nonetheless, apatite crystals in Cluster B garnets (figure 12B) have shown a characteristic greenish color, xenomorphic shape, and lack of graphite inclusions (Gilg et al., 2010), an appearance distinct from that of apatite in the engraved gem and the Garibpet garnets.

Monazite and zircon inclusions have been noted in all different types of almandines discussed in this paper. A three-dimensional network of rutile inclusions (figure 12A,C) has only very rarely been observed in Cluster B garnets but has occurred commonly in Cluster A garnets (Calligaro et al., 2002, 2006-2007; Gilg et al., 2010; Gast et al., 2013). Brownish biotite inclusions have so far only been detected in Cluster A garnets by scanning electron microscopy (Horváth and Bendö, 2011). Uraninite inclusions have been reported as a typical feature only of Cluster B garnets (figure 12D; Calligaro et al., 2002, 2006-2007).

Although certain mineral inclusion features of the engraved gem can be observed in either of the two Ca-poor almandine types in Merovingian jewelry, on balance the combination of features is quite distinctive and consistent only with garnets from the Garibpet deposit. In particular, the sillimanite fibers at the border between an inclusion-rich core and an inclusion-poor rim and the long-prismatic graphite-bearing apatite crystals can be considered the most distinguishing inclusion characteristics.

DISCUSSION AND CONCLUSIONS

Schmetzer et al. (2017) proposed that assignment of garnet samples from a historical context to a specific garnet type or cluster used in antiquity should ideally be based on a series of criteria. For instance:

1. Major element chemical composition, including proportions of garnet end members
2. Chemical zoning for major and minor elements within the crystals from core to rim
3. Trace-element contents
4. Zoning of trace elements from core to rim
5. General inclusion assemblage
6. Appearance of individual inclusions
7. Distribution and zoning of inclusions

It was emphasized that a detailed correlation of several features, rather than merely one or two, should

be considered a prerequisite for assigning a sample to an established garnet type or cluster.

Here, the present study has demonstrated that the engraved gemstone and samples from the Garibpet deposit are consistent with respect to six of the seven criteria just mentioned, namely 1–3 and 5–7. Examining trace-element zoning in the gem was not possible due to experimental restrictions.

Only one inclusion characteristic was not entirely congruent: the absence of thick acicular sillimanite needles in the engraved gemstone. The thick acicular sillimanite needles were observed only in about 10% of Garibpet garnets, however. This is understandable, since garnets from different areas of the large deposit, mined during different historical eras, might also show a degree of variability.

Thus, being unaware of any other known deposit with garnets showing the characteristic features described for the Garibpet material, the authors conclude that the Early Byzantine garnet engraved with a Christian motif originated from this secondary deposit. Garnets from the Garibpet deposit were used extensively for the historical bead-making industry of Arikamedu, in Tamil Nadu State. The bead enterprise flourished from the second century BCE at least until the end of the first millennium CE and probably even to the early seventeenth century (Begley et al., 2004; Francis, 2002, 2004; Schmetzer et al., 2017). The examined spherical and faceted bicone garnet beads from the Arikamedu archaeological site had diameters of less than 5.5 mm, in contrast to the 11 mm length of the engraved gemstone. Nonetheless, rough fragments from Arikamedu reaching 11 mm in size were observed during the 2017 investigation, and material even exceeding that size was found at the Garibpet deposit (Schmetzer et al., 2017).

Accordingly, the present study can be considered to offer the first strong, tangible evidence of garnet trading from the eastern coast of India to the Mediterranean realm, including the Byzantine Empire, in the late sixth to eighth century CE, even as use of garnet for cloisonné jewelry in central Europe declined (for details see Schmetzer et al., 2017, p. 599). When such evidence is combined with the recent work demonstrating use of Garibpet material for bead-making at Arikamedu, the shipment of garnet rough or beads from Arikamedu or nearby harbors on the Coromandel Coast can logically be assumed. Doing so is also consistent with prior interpretation of the sixth-century text by Cosmas Indicopleustes regarding export of "alabandenum" to the Mediterranean region from a port named "Caber," as referring to garnets shipped from Kaveripattinam, close to Arikamedu. Hence, the idea that garnets were transported and traded from Indian ports along the so-called Maritime Silk Road, which connected China with the Western world, becomes a supportable proposition.

It should be noted, however, that the vast majority of almandine garnets that were used for Merovingian cloisonné jewelry and supposedly derived from an Indian source (Greiff, 1998; Quast and Schüssler, 2000; Calligaro et al., 2002, 2006-2007; Gilg et al., 2010; Périn and Calligaro, 2016) must have originated from different localities and likely were not traded from the Coromandel Coast.

Lastly, as a practical point, this study further demonstrates that chemical analysis of ancient garnets using a portable X-ray fluorescence instrument with helium flow mode, in combination with microscopic investigations, can be sufficient to assign a gemstone to a known almandine type or cluster, despite the relatively low precision of the XRF technique for some major elements, (e.g., Fe, Si, Al, and Mg). Specifically, the capability of the device to measure important minor elements including Mn, Ca, and to a lesser extent Mg, as well as the characteristic trace elements Y, Cr, and Zn, provides adequate data. Thus, this research may encourage other scientists to augment the information compiled to date on historical gemstones and their trading.

ABOUT THE AUTHORS

Prof. Gilg is a professor at the Chair of Engineering Geology, Technical University of Munich, Germany. Dr. Schmetzer is an independent researcher living in Petershausen, near Munich. Prof. Schüssler is affiliated with the Institute for Geography and Geology, Würzburg University, Germany.

ACKNOWLEDGMENTS

The authors would like to thank Dr. Christian Schmidt of Munich for the opportunity to analyze engraved garnets from his collection with non-destructive methods. Prof. R. Gebhard (Archäologische Staatssammlung, Munich) provided access to the portable X-ray fluorescence instrument.

REFERENCES

Adams N. (2011) The garnet millennium: The role of seal stones in garnet studies. In C. Entwistle and N. Adams, Eds., *'Gems of Heaven': Recent Research on Engraved Gemstones in Late Antiquity c. AD 200–600*. British Museum Research Publication 177, The British Museum, London, pp. 10–24.

——— (2014) *Bright Lights in the Dark Ages: The Thaw Collection of Early Medieval Ornaments*. D. Giles Ltd, London, 408 pp.

Adams N., Lüle C., Passmore E. (2011) Lithois Indikois: Preliminary characterisation of some garnet seal stones from Central and South Asia. In C. Entwistle and N. Adams, Eds., *'Gems of Heaven': Recent Research on Engraved Gemstones in Late Antiquity c. AD 200–600*. British Museum Research Publication 177, The British Museum, London, pp. 25–38.

Arrhenius B. (1985) *Merovingian Garnet Jewellery: Emergence and Social Implications*. Almqvist och Wiksell International, Stockholm, 229 pp.

Banaji J. (2015) "Regions that look seaward": Changing fortunes, submerged histories and the slow capitalism of the sea. In M. Maiuro and F. De Romanis, Eds., *Across the Ocean: Nine Chapters on Indo-Mediterranean Trade*. Brill, Leiden, the Netherlands pp. 114–126.

Bauer M. (1896) *Edelsteinkunde*. Chr. Herm. Tauchnitz, Leipzig, Germany pp. 400–404.

Begley V., Francis P., Jr., Mahadevan I., Raman K.V., Sidebotham S.E., Slane K.W., Will E.L. (1996) *The Ancient Port of Arikamedu. New Excavations and Researches 1989-1992, Volume One*. École Française d'Extrême-Orient, Pondicherry, India, 400 pp.

Begley V., Francis P., Jr., Raman K.V., Sidebotham S.E., Will E.L. (2004) *The Ancient Port of Arikamedu: New Excavations and Researches, 1989-1992, Vol. 2*. École Française d'Extrême-Orient, Paris, 644 pp.

Beyssac O., Goffé B., Chopin C., Rouzaud J.N. (2002) Raman spectra of carbonaceous material in metasediments: A new geothermometer. *Journal of Metamorphic Geology*, Vol. 20, No. 9, pp. 859–871, http://dx.doi.org/10.1046/j.1525-1314.2002.00408.x

Borell B. (2017) Gemstones in southeast Asia and beyond: Trade along the maritime networks. In A. Hilgner, D. Quast, and S. Greiff, Eds., *Gemstones in the First Millennium AD: Mines, Trade, Workshops and Symbolism*. RGZM Tagungen Vol. 30, Verlag des Römisch-Germanischen Zentralmuseums, Mainz, pp. 21–44.

Brubaker L. (2012) *Inventing Byzantine Iconoclasm*. Bristol Classical Press, London, 134 pp.

Brubaker L., Haldon J. (2001) *Byzantium in the Iconoclast Era (ca 680–850): The Sources: An Annotated Survey*. Ashgate Publishing, Aldershot, UK, 324 pp.

Bugoi R., Oanţâ-Marghitu R., Calligaro T. (2016) IBA investigations of loose garnets from Pietroasa, Apahida and Cluj-Someşeni treasures (5th century AD). *Nuclear Instruments and Methods in Physics Research B*, Vol. 371, pp. 401–406, http://dx.doi.org/10.1016/j.nimb.2015.09.038

Calligaro T., Colinart S., Poirot J.-P., Sudres C. (2002) Combined external-beam PIXE and μ-Raman characterisation of garnets used in Merovingian jewellery. *Nuclear Instruments and Methods in Physics Research B*, Vol. 189, No. 1-4, pp. 320–327, http://dx.doi.org/10.1016/S0168-583X(01)01078-3

Calligaro T., Périn P., Vallet F., Poirot J.-P. (2006-2007) Contribution á l'étude des grenats mérovingiens (Basilique de Saint-Denis et autres collections du musée d'Archéologie nationale, diverses collections publiques et objects de fouilles récentes). *Antiquités Nationales*, Vol. 38, pp. 111–144.

Carter A.K. (2012) Garnet beads in Southeast Asia: Evidence for local production? In M.-L. Tjoa-Bonatz, A. Reinecke, and D. Bonatz, Eds., *Crossing Borders: Selected Papers from the 13th International Conference of the European Association of Southeast Asian Archaeologists, Volume 1*. NUS Press, Singapore, pp. 296–306.

——— (2013) Trade, exchange, and socio-political development in Iron Age (500 BC–AD 500) mainland southeast Asia: An examination of stone and glass beads from Cambodia and Thailand. Unpublished PhD dissertation, Department of Anthropology, University of Wisconsin-Madison.

——— (2016) Determining the provenience of garnet beads using LA-ICP-MS. In L. Dussubieux, M. Golitko, and B. Gratuze, Eds., *Recent Advances in Laser Ablation ICP-MS for Archaeology*. Springer, Vienna, pp. 235–266.

Casal J.M. (1949) *Fouilles de Virampatnam-Arikamedu*. Imprimerie Nationale, Paris, 71 pp.

Entwistle C., Adams N. (2011) *'Gems of Heaven': Recent Research on Engraved Gemstones in Late Antiquity c. AD 200–600*. British Museum Research Publication 177, The British Museum, London.

Francis P., Jr. (2002) *Asia's Maritime Bead Trade: 300 B.C. to the Present*. University of Hawai'i Press, Honolulu, 305 pp.

——— (2004) Beads and selected small finds from the 1989-92 excavations. In V. Begley et al., Eds., *The Ancient Port of Arikamedu: New Excavations and Researches, 1989-1992, Volume Two*. École Française d'Extrême-Orient, Paris, pp. 447–604.

Gast N., Calligaro T., Gilg H.A., Macknapp K., Schmahl W.W., Stark R. (2013) Die Funde: Farbige Einlagen. In R. Gebhard and B. Haas-Gebhard, Eds., *Unterhaching. Eine Grabgruppe der Zeit um 500 n. Chr. bei München*. Abhandlungen und Bestandskataloge der Archäologischen Staatssammlung München, Vol. 1, pp. 50–74.

Gaur A.S., Sundaresh (2006) Onshore and near shore explorations along the southern Tamilnadu coast: With a view to locating ancient ports and submerged sites. In P.C. Reddy, Ed., *Mahasenasiri: Riches of Indian Archaeological and Cultural Studies*. Sharda Publishing House, New Delhi, pp. 122–130.

Gilg H.A., Gast N. (2012) Naturwissenschaftliche Untersuchungen an Granatgemmen der Sammlung James Loeb. In F. Knauß, Ed., *Die Gemmen der Sammlung James Loeb, Forschungen der Staatlichen Antikensammlung und Glyptothek*, Supplement zu Band 1. Kunstverlag J. Fink, Lindenberg im Allgäu, pp. 48–57, 62–63.

Gilg H.A., Hyršl J. (2014) Garnet deposits in Europe. In J. Toussaint, Ed., *Rouges et Noirs. Rubies, grenat, onyx, obsidienne et autres minéraux rouges et noirs dans l'art et l'archéologie*. Monographies du Musée Provincial des Arts du Namurois-Trésor d'Oignies (TreM.a), Société Archéologique de Namur, Namur, pp. 144–173.

Gilg H.A., Gast N., Calligaro T. (2010) Vom Karfunkelstein. In L. Wamser, Ed., *Karfunkelstein und Seide*. Ausstellungskataloge der Archäologischen Staatssammlung (München), Band 37, pp. 87–100.

Greiff S. (1998) Naturwissenschaftliche Untersuchungen zur Frage der Rohsteinquellen für frühmittelalterlichen Almandingranatschmuck rheinfränkischer Provenienz. *Jahrbuch des Römisch-Germanischen Zentralmuseums Mainz*, Vol. 45, No. 2, pp. 599–646.

Horváth E., Bendö Z. (2011) Provenance study on a collection of loose garnets from a Gepidic period grave in Northeast Hungary. *Archeometriai Mühely*, Vol. 2011, No. 1, pp. 17–32.

Kessler O. (2001) Der spätantik-frühmittelalterliche Handel zwischen Europa und Asien und die Bedeutung des Almandins als Fernhandelsgut. In *Archäologisches Zellwerk: Beiträge zur Kulturgeschichte in Europa und Asien*; Internationale Archäologie: Studia honoraria, Vol. 16, Verlag Marie Leidorf, Rahden, pp. 113–128.

Locock A.J. (2008) An Excel spreadsheet to recast analyses of garnet into end-member components, and a synopsis of the crystal

chemistry of natural silicate garnets. *Computers & Geosciences*, Vol. 34, No. 12, pp. 1769–1780, http://dx.doi.org/10.1016/j.cageo.2007.12.013
Löfgren J. (1973) Die mineralogische Untersuchung der Granaten von Paviken auf Gotland. *Early Medieval Studies*, Vol. 6, No. 9, pp. 78–96.
Mannerstrand M., Lundqvist L. (2003) Garnet chemistry from the Slöinge excavation, Halland and additional Swedish and Danish excavations—Comparisons with garnet occurring in a rock context. *Journal of Archaeological Science*, Vol. 30, No. 2, pp. 169–183, http://dx.doi.org/10.1006/jasc.2000.0583
Mathis F., Vrielynck O., Laclavetine K., Chêne G., Strivay D. (2008) Study of the provenance of Belgian Merovingian garnets by PIXE at IPNAS cyclotron. *Nuclear Instruments and Methods in Physics Research B*, Vol. 266, No. 10, pp. 2348–2352, http://dx.doi.org/10.1016/j.nimb.2008.03.055
Mirza K. (1937) A brief outline of Hyderabad State with a reference to its mineral resources. *Hyderabad Geological Series Bulletin*, No. 2, p. 39.
Périn P., Calligaro T. (2007) Neue Erkenntnisse zum Arnegundegrab. Ergebnisse der Metallanalysen und der Untersuchungen organischer Überreste aus Sarkophag 49 aus der Basilika von Saint-Denis. *Acta Praehistorica et Archaeologica*, Vol. 39, pp. 147–179.
——— (2016) Note sur l'origine des grenats utilises par les orfèvres du haut Moyen Âge occidental européen. In Á. Bollók, G. Csiky, and T. Vida, Eds., *Between Byzantium and the Steppe: Archaeological and Historical Studies in Honour of Csanád Bálint on the Occasion of His 70th Birthday*. MTA BTK Régészeti Intézet, Budapest, pp. 75–85.
Phani P.R. (2014) Mineral resources of Telangana State, India: The way forward. *International Journal of Innovative Research in Science, Engineering and Technology*, Vol. 3, No. 8, pp. 15450–15459, http://dx.doi.org/10.15680/IJIRSET.2014.0308052
Ptak R. (2007) *Die maritime Seidenstrasse*. Verlag C.H. Beck, Munich, 368 pp.
Quast D., Schüssler U. (2000) Mineralogische Untersuchungen zur Herkunft der Granate merowingerzeitlicher Cloisonnéarbeiten. *Germania*, Vol. 78, No. 1, pp. 75–96.
Raman K.V. (1991) Further evidence of Roman trade from costal sites in Tamil Nadu. In V. Begley and R.D. De Puma, Eds., *Rome and India: The Ancient Sea Trade*. University of Wisconsin Press, Madison, pp. 125–133.
Rao S.R (1991a) Underwater exploration of submerged towns near Tranquebar (Tarangambadi) on Tamilnadu coast. In S.R. Rao, Ed., *Recent Advances in Marine Archaeology*. Society for Marine Archaeology, Goa, India pp. 60–64.
——— (1991b) Marine archaeological explorations of Tranquebar-Poompuhar region on Tamil Nadu coast. *Marine Archaeology*, Vol. 2, pp. 5–20.
Ritter N.C. (2017) Gemstones in pre-Islamic Persia: social and symbolic meanings of Sasanian seals. In A. Hilgner, D. Quast, and S. Greiff, Eds., *Gemstones in the First Millennium AD: Mines, Trade, Workshops and Symbolism*. RGZM Tagungen Vol. 30, Verlag des Römisch-Germanischen Zentralmuseums, Mainz, Germany, pp. 277–292.
Roth H. (1980) Almandinhandel und -verarbeitung im Bereich des Mittelmeeres. *Allgemeine und vergleichende Archaeologie*, Vol. 2, pp. 309–333.
Schmetzer K., Gilg H.A., Schüssler U., Panjikar J., Calligaro T., Périn P. (2017) The linkage between garnets found in India at the Arikamedu archaeological site and their source at the Garibpet deposit. *Journal of Gemmology*, Vol. 35, No. 7, pp. 598–627.
Schneider H. (2011) K*osmas Indikopleustes, Christliche Topographie: Textkritische Analysen. Übersetzung. Kommentar*. Brepols Publishers, Turnhout, Belgium, 298 pp.
Šmit Ž., Fajfar H., Jeršek M., Knific T., Lux J. (2014) Analysis of garnets from the archaeological sites in Slovenia. *Nuclear Instruments and Methods in Physics Research B*, Vol. 328, pp. 89–94, https//dx.doi.org/10.1016/j.nimb.2014.02.121
Spear F.S. (1993) *Metamorphic Phase Equilibria and Pressure-Temperature-Time Paths*. Mineralogical Society of America, Washington, DC, 799 pp.
Spier J. (1989) A group of Ptolemaic engraved garnets. *Journal of the Walters Art Gallery*, Vol. 47, pp. 67–80.
——— (2007) *Late Antique and Early Christian Gems*. Reichert Verlag, Wiesbaden, 221 pp.
——— (2011) Late antique gems: Some unpublished examples. In C. Entwistle and N. Adams, Eds., *'Gems of Heaven': Recent Research on Engraved Gemstones in Late Antiquity c. AD 200–600*. British Museum Research Publication 177, The British Museum, London, pp. 193–207.
Sundaresh, Gaur A.S. (2011) Marine archaeological investigations on Tamil Nadu coast, India: An overview. In M. Staniforth et al., Eds., *Proceedings of the 2011 Asia-Pacific Regional Conference on Underwater Cultural Heritage*. Asian Academy for Heritage Management, pp. 233–248.
Thoresen L. (2017) Archeogemmology and ancient literary sources on gems and their origins. In A. Hilgner, D. Quast, and S. Greiff, Eds., *Gemstones in the First Millennium AD: Mines, Trade, Workshops and Symbolism*. RGZM Tagungen Vol. 30, Verlag des Römisch-Germanischen Zentralmuseums, Mainz, Germany, pp. 155–218.
Thoresen L., Schmetzer K. (2013) Greek, Etruscan and Roman garnets in the antiquities collection of the J. Paul Getty Museum. *Journal of Gemmology*, Vol. 33, No. 7-8, pp. 201–222.
Voysey H.W. (1833) Second report on the geology of Hyderabad. *Journal of the Asiatic Society of Bengal*, Vol. 2, No. 20, pp. 392–405.
Wang A., Freeman J.J., Jolliff, B.L. (2015) Understanding the Raman spectral features of phyllosilicates. *Journal of Raman Spectroscopy*, Vol. 46, No. 10, pp. 829–845, http://dx.doi.org/10.1002/jrs.4680
Wheeler R.E.M., Ghosh A., Deva K. (1946) Arikamedu: An Indo-Roman trading-station on the east coast of India. *Ancient India*, No. 2, pp. 17–124.
Winstedt E.O. (1909) *The Christian Topography of Cosmas Indicopleustes*. Cambridge University Press, Edinburgh, UK, 376 pp.
Wopenka B., Pasteris J.D. (1993) Structural characterization of kerogens to granulite-facies graphite: Applicability of Raman microprobe spectroscopy. *American Mineralogist*, Vol. 78, No. 5-6, pp. 533–557
Zwierlein-Diehl E. (2007) *Antike Gemmen und ihr Nachleben*. Walter de Gruyter, Berlin/New York, 567 pp.